The final stages of stellar evolution

11th Symposium on Nuclei in the Cosmos (NIC XI)

Heidelberg, 19-23 July 2010

Alessandro Chieffi

Istituto Nazionale di AstroFisica (Istituto di Astrofisica Spaziale e Fisica Cosmica)

&

Centre for Stellar and Planetary Astrophysics – Monash University - Australia

Email: alessandro.chieffi@iasf-roma.inaf.it

Marco Limongi

Istituto Nazionale di AstroFisica (Osservatorio Astronomico di Roma)

&

Centre for Stellar and Planetary Astrophysics – Monash University - Australia

Email: marco@oa-roma.inaf.it

Istituto di Astrofisica Spaziale e Fisica Cosmica - Roma

MONASH UNIVERSITY

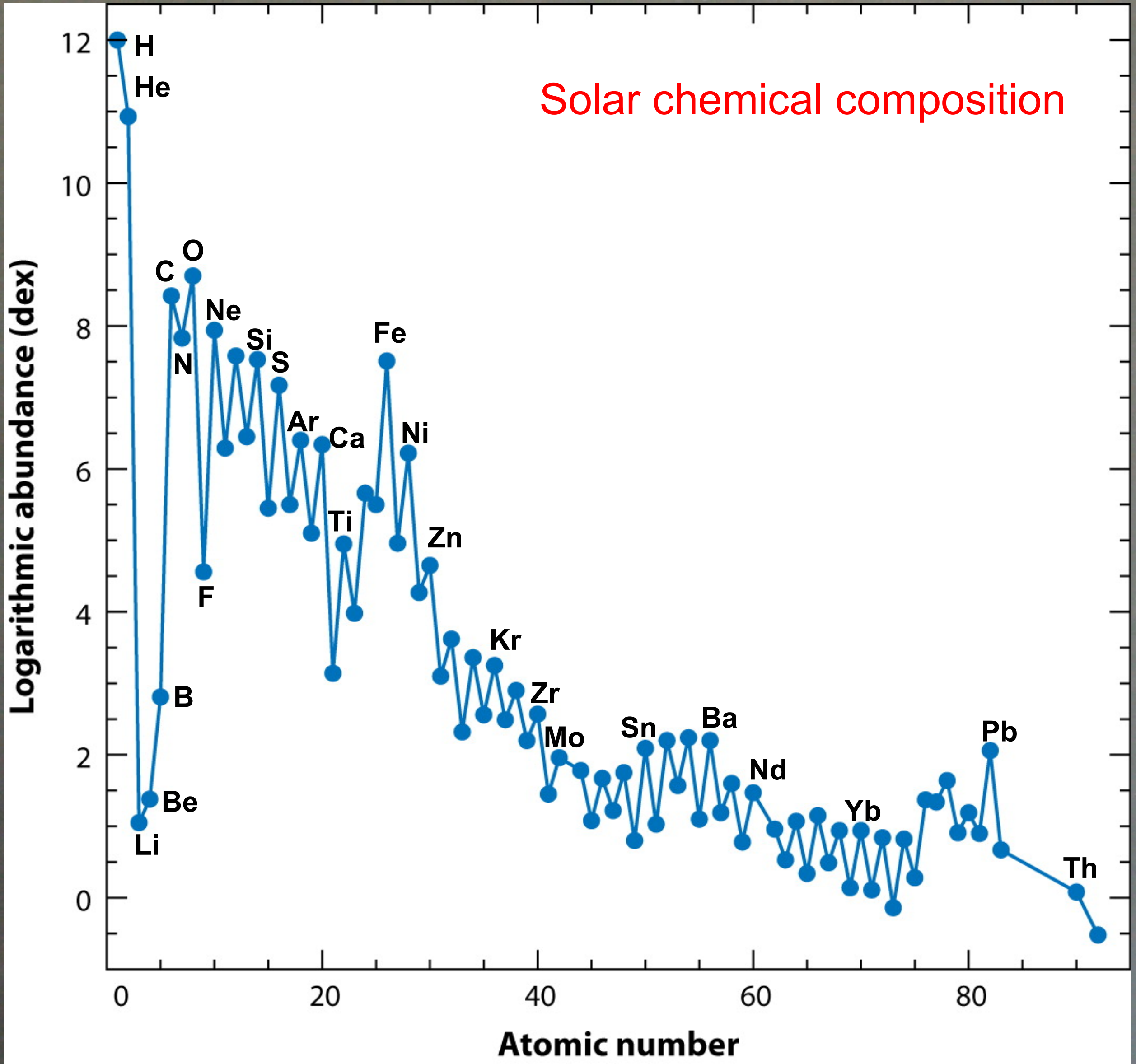

Asplund M, et al. 2009.
Annu. Rev. Astron. Astrophys. 47:481–522

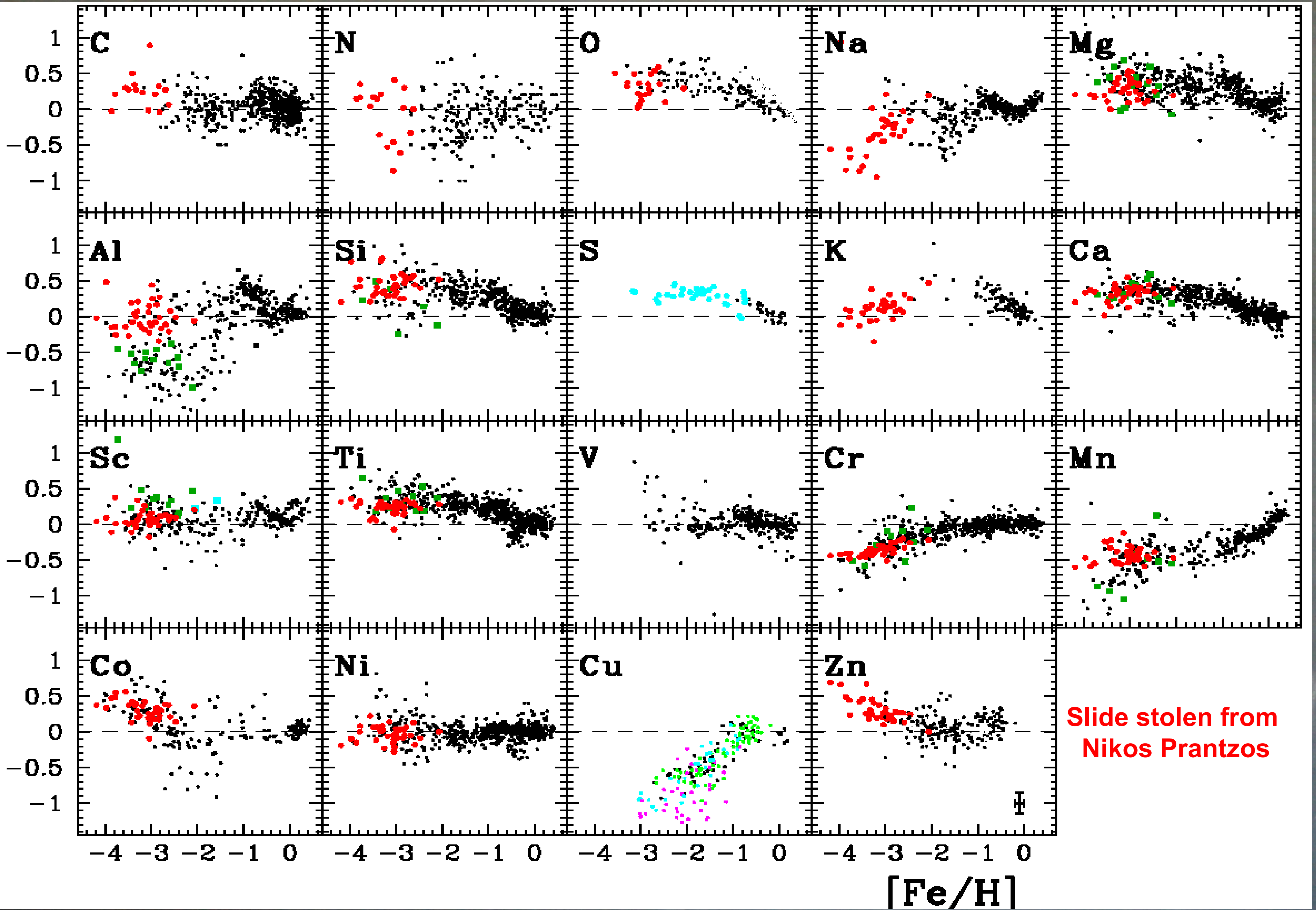
C
N
O
Na
Mg
Al
Si
S
K
Ca
Sc
Ti
V
Cr
Mn
Co
Ni
Cu
Zn
1
0.5
0
−0.5
−1
−4 −3 −2 −1 0
[Fe/H]
Slide stolen from
Nikos Prantzos

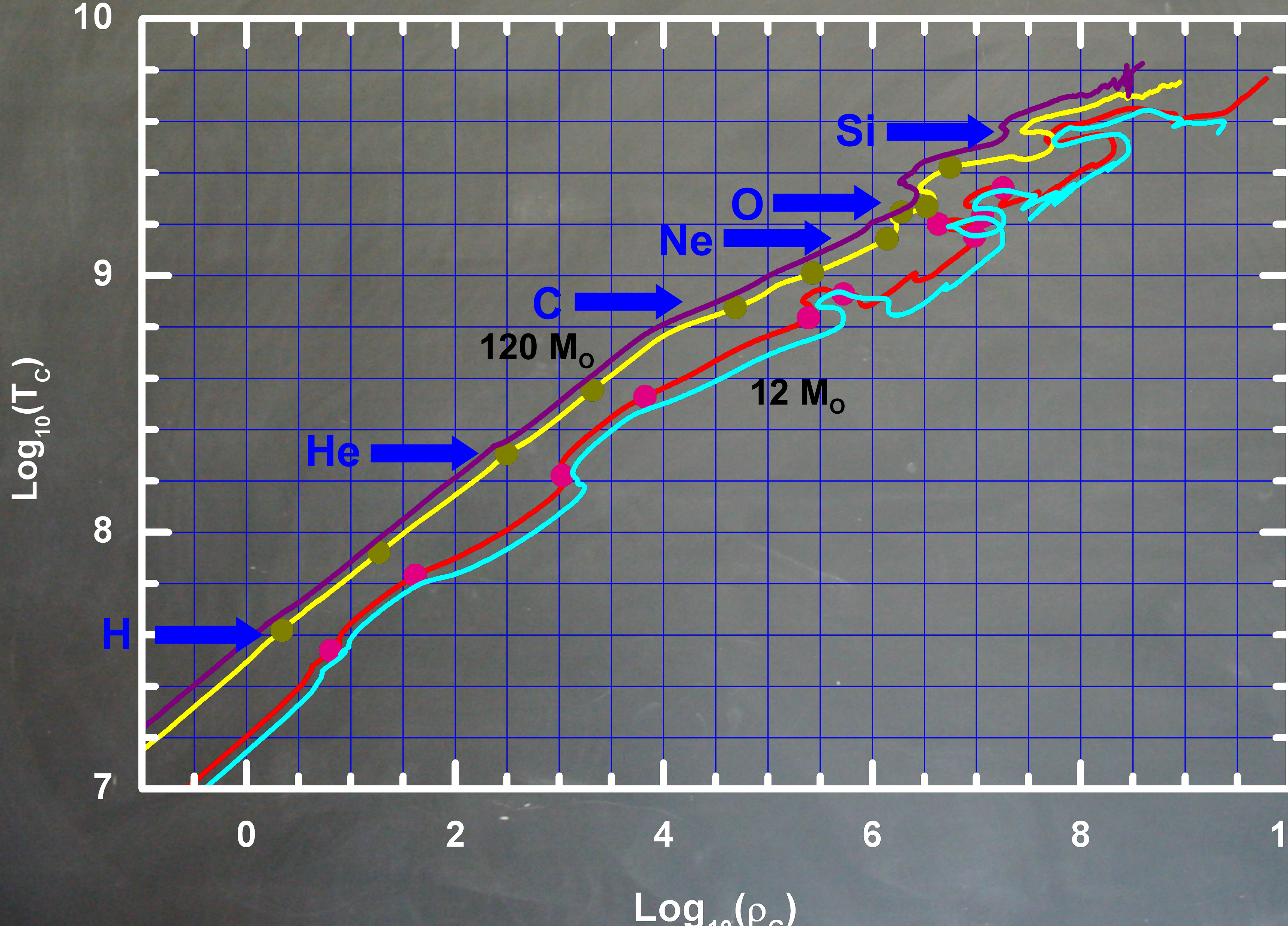

10
9
8
7
Log10(TC)
0
2
4
6
8
10
Log10(ρC)
H
He
C
Ne
O
Si
120 MO
12 MO

Convective zones

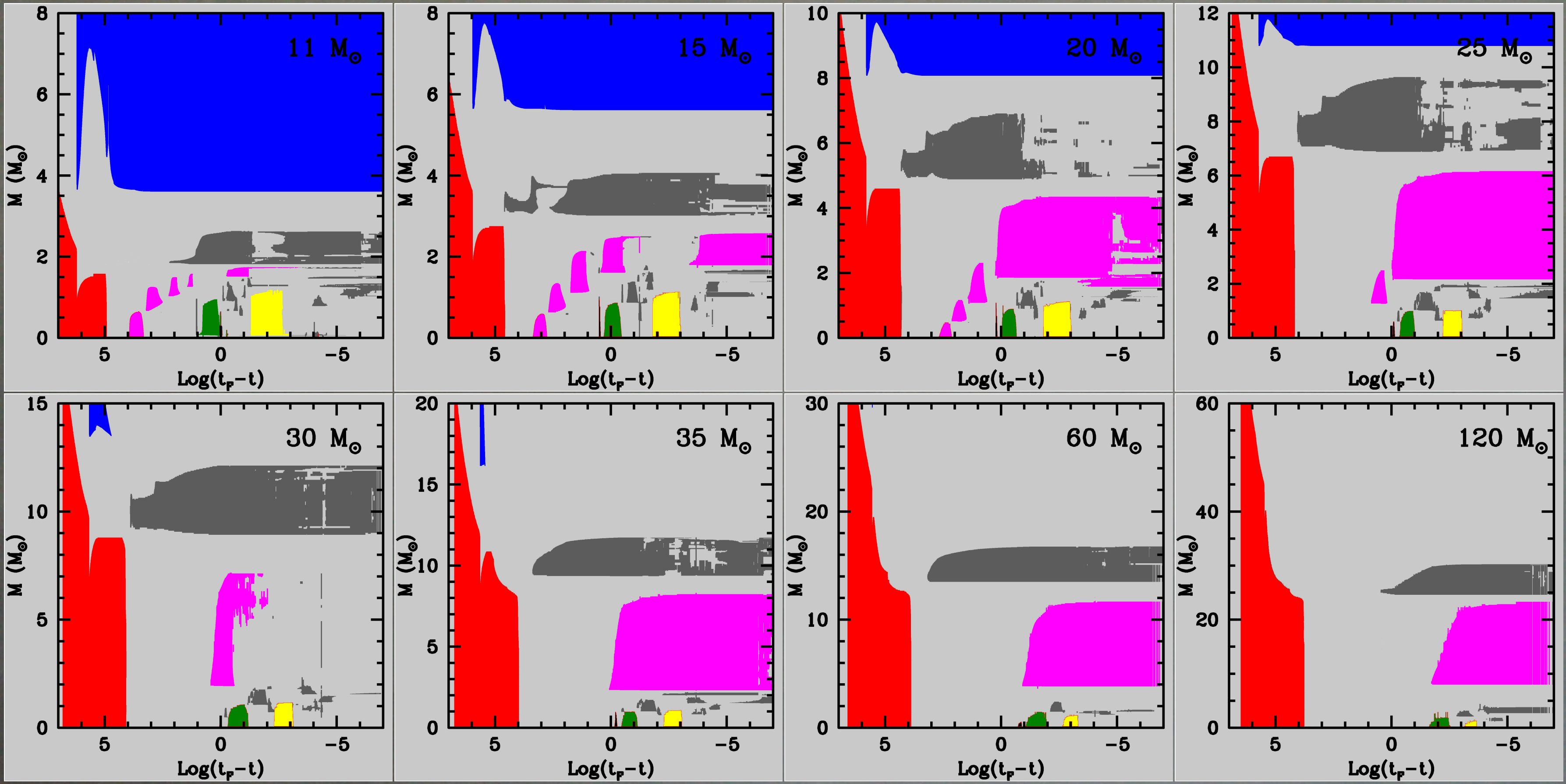

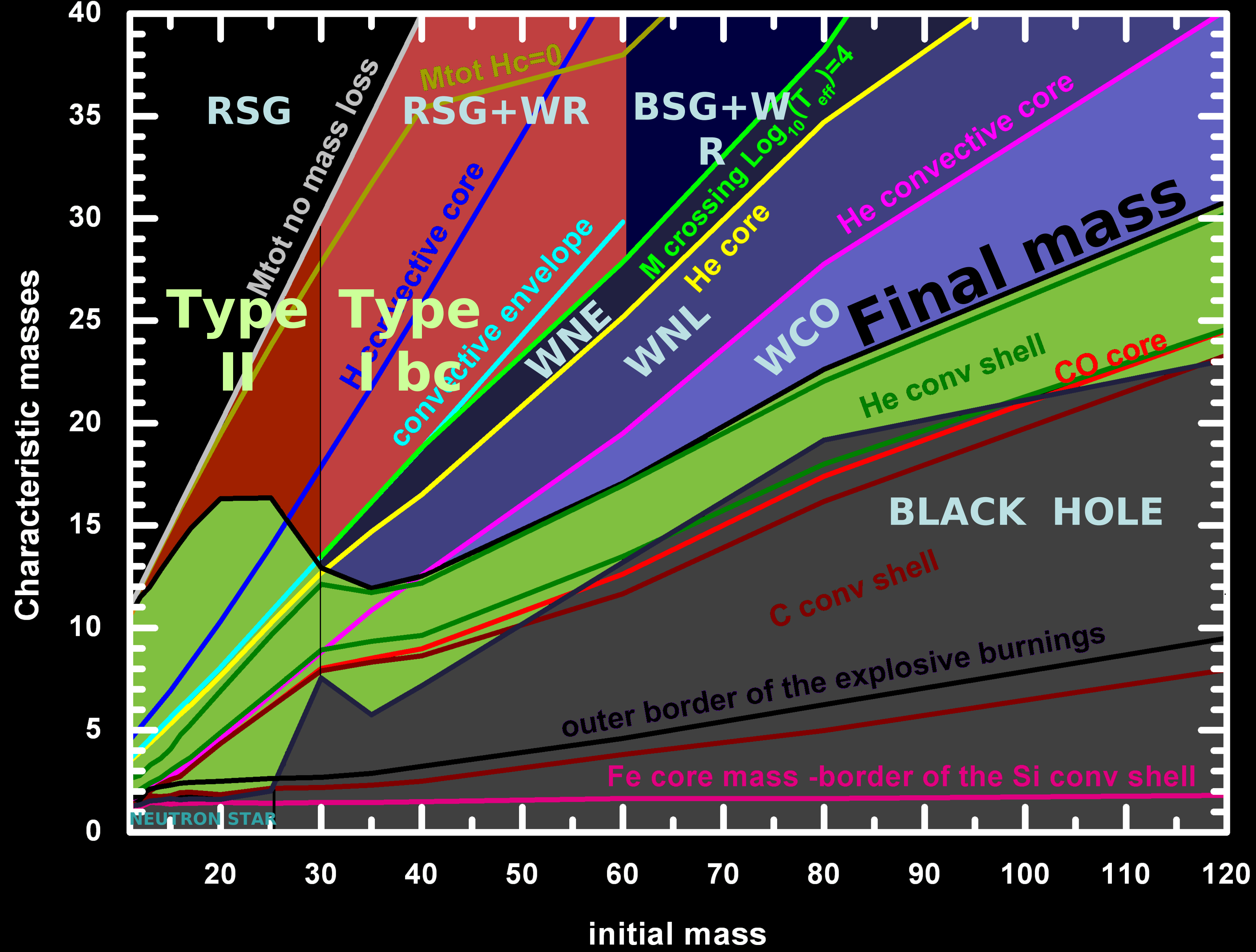

RSG
RSG+WR
BSG+WR
Mtot no mass loss
Mtot Hc=0
H convective core
convective envelope
M crossing Log10(T eff)=4
He core
He convective core
Type II
Type I bc
WNE
WNL
WCO
Final mass
He conv shell
CO core
BLACK HOLE
C conv shell
outer border of the explosive burnings
Fe core mass -border of the Si conv shell
NEUTRON STAR
Characteristic masses
initial mass
0
5
10
15
20
25
30
35
40
20
30
40
50
60
70
80
90
100
110
120

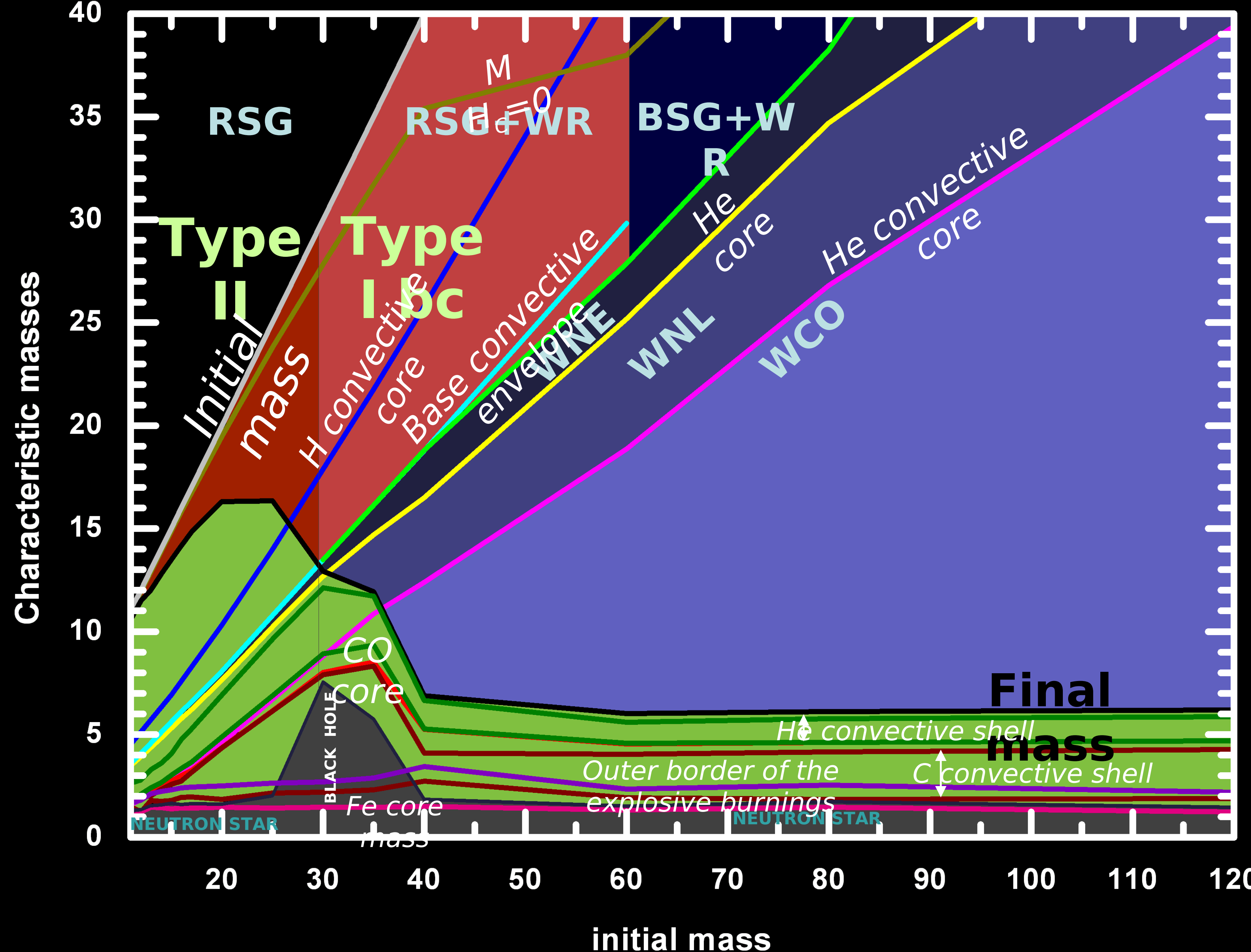
RSG
RSG+WR
BSG+WR
M H=0
Type II
Type I bc
Initial mass
H convective core
Base convective envelope
WNE
WNL
WCO
He core
He convective core
CO core
BLACK HOLE
Fe core mass
NEUTRON STAR
He convective shell
C convective shell
Outer border of the explosive burnings
Final mass
Characteristic masses
initial mass
0
5
10
15
20
25
30
35
40
20
30
40
50
60
70
80
90
100
110
120

1 foe

Mass Loss in the WNE / WCO phases: Langer89 - Nugis & Lamers 00

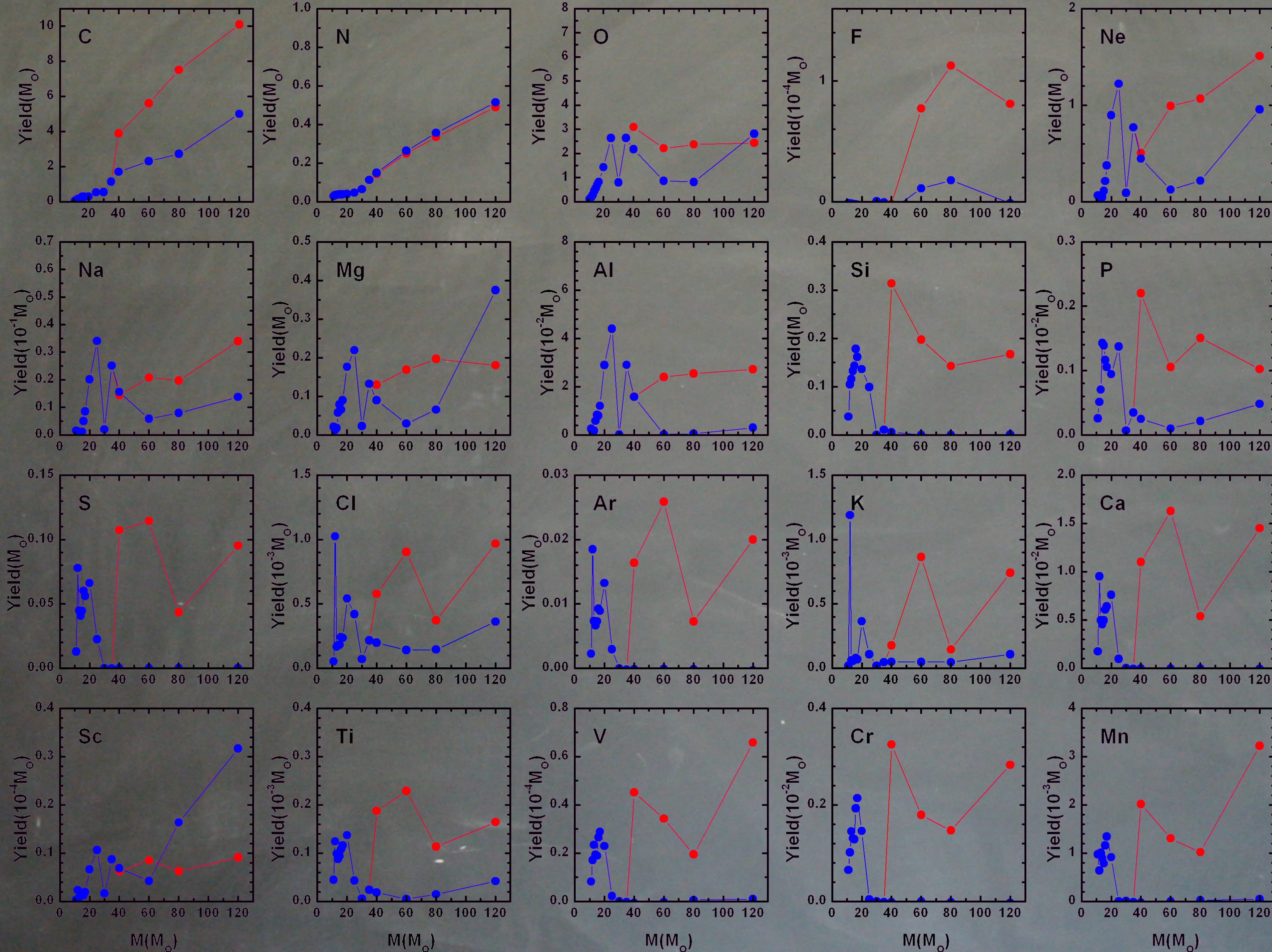

Mass Loss in the WNE / WCO phases: Langer89 - Nugis & Lamers 00

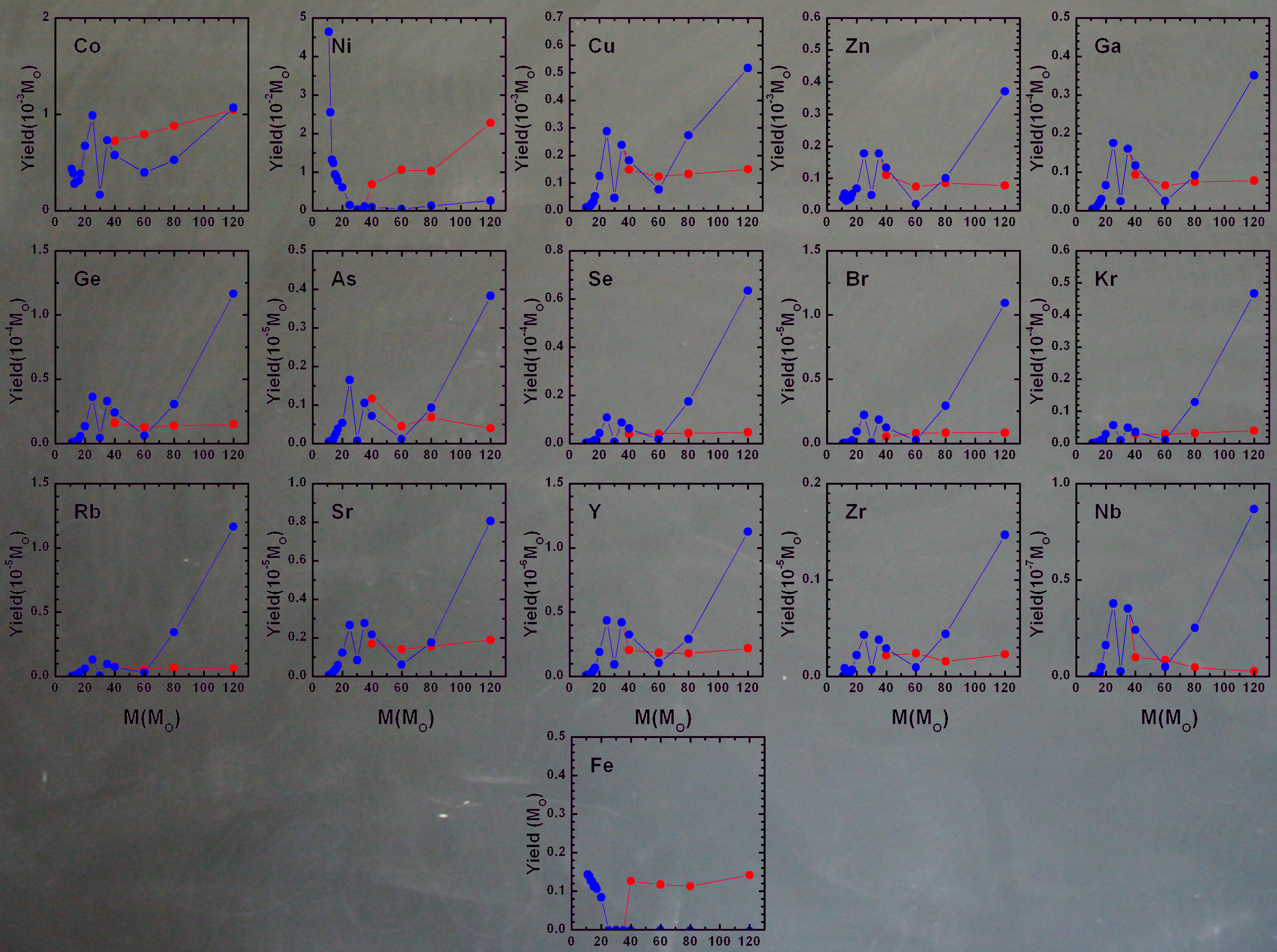

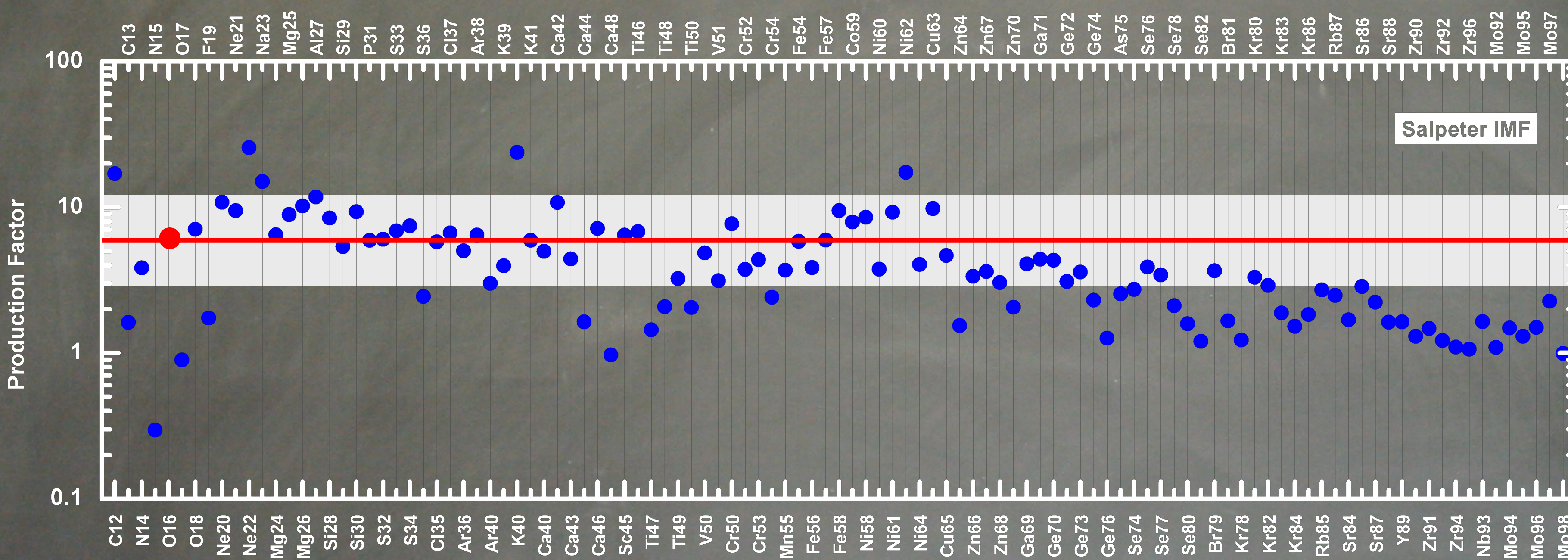

Production Factor
Salpeter IMF
100
10
1
0.1
C13 N15 O17 F19 Ne21 Na23 Mg25 Al27 Si29 P31 S33 S36 Cl37 Ar38 K39 K41 Ca42 Ca44 Ca48 Ti46 Ti48 Ti50 V51 Cr52 Cr54 Fe54 Fe57 Co59 Ni60 Ni62 Cu63 Zn64 Zn67 Zn70 Ga71 Ge72 Ge74 As75 Se76 Se78 Se82 Br81 Kr80 Kr83 Kr86 Rb87 Sr86 Sr88 Zr90 Zr92 Zr96 Mo92 Mo95 Mo97
C12 N14 O16 O18 Ne20 Ne22 Mg24 Mg26 Si28 Si30 S32 S34 Cl35 Ar36 Ar40 K40 Ca40 Ca43 Ca46 Sc45 Ti47 Ti49 V50 Cr50 Cr53 Mn55 Fe56 Fe58 Ni58 Ni61 Ni64 Cu65 Zn66 Zn68 Ga69 Ge70 Ge73 Ge76 Se74 Se77 Se80 Br79 Kr78 Kr82 Kr84 Rb85 Sr84 Sr87 Y89 Zr91 Zr94 Nb93 Mo94 Mo96 Mo98

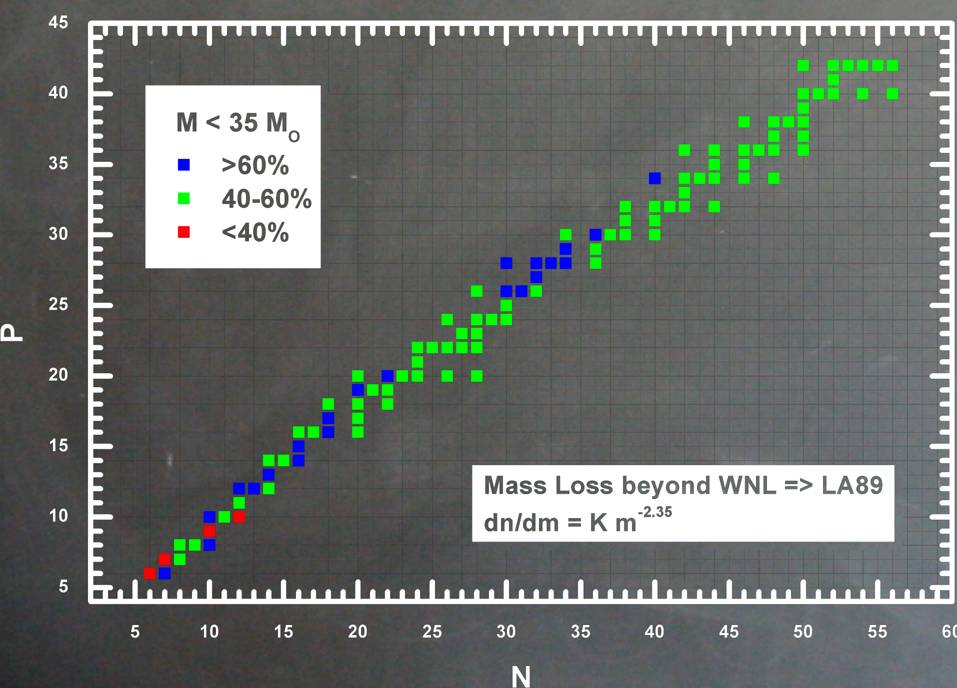

M < 35 M$_O$
>60%
40-60%
<40%
Mass Loss beyond WNL => LA89
dn/dm = K m$^{-2.35}$
P
N
45 40 35 30 25 20 15 10 5
5 10 15 20 25 30 35 40 45 50 55 60

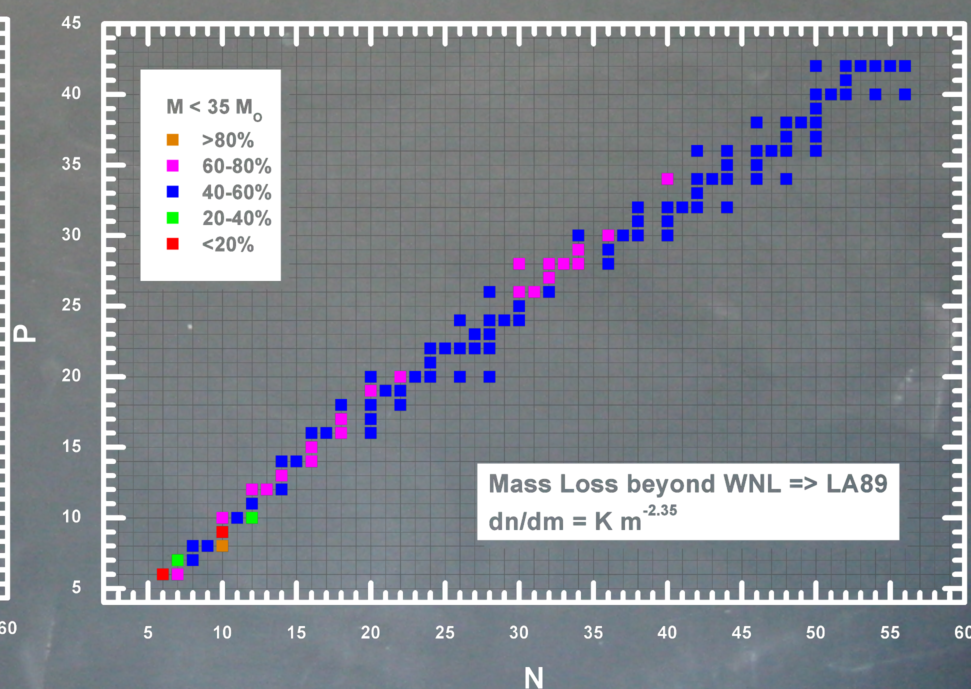

M < 35 M$_O$
>80%
60-80%
40-60%
20-40%
<20%
Mass Loss beyond WNL => LA89
dn/dm = K m$^{-2.35}$
P
N
45 40 35 30 25 20 15 10 5
5 10 15 20 25 30 35 40 45 50 55 60

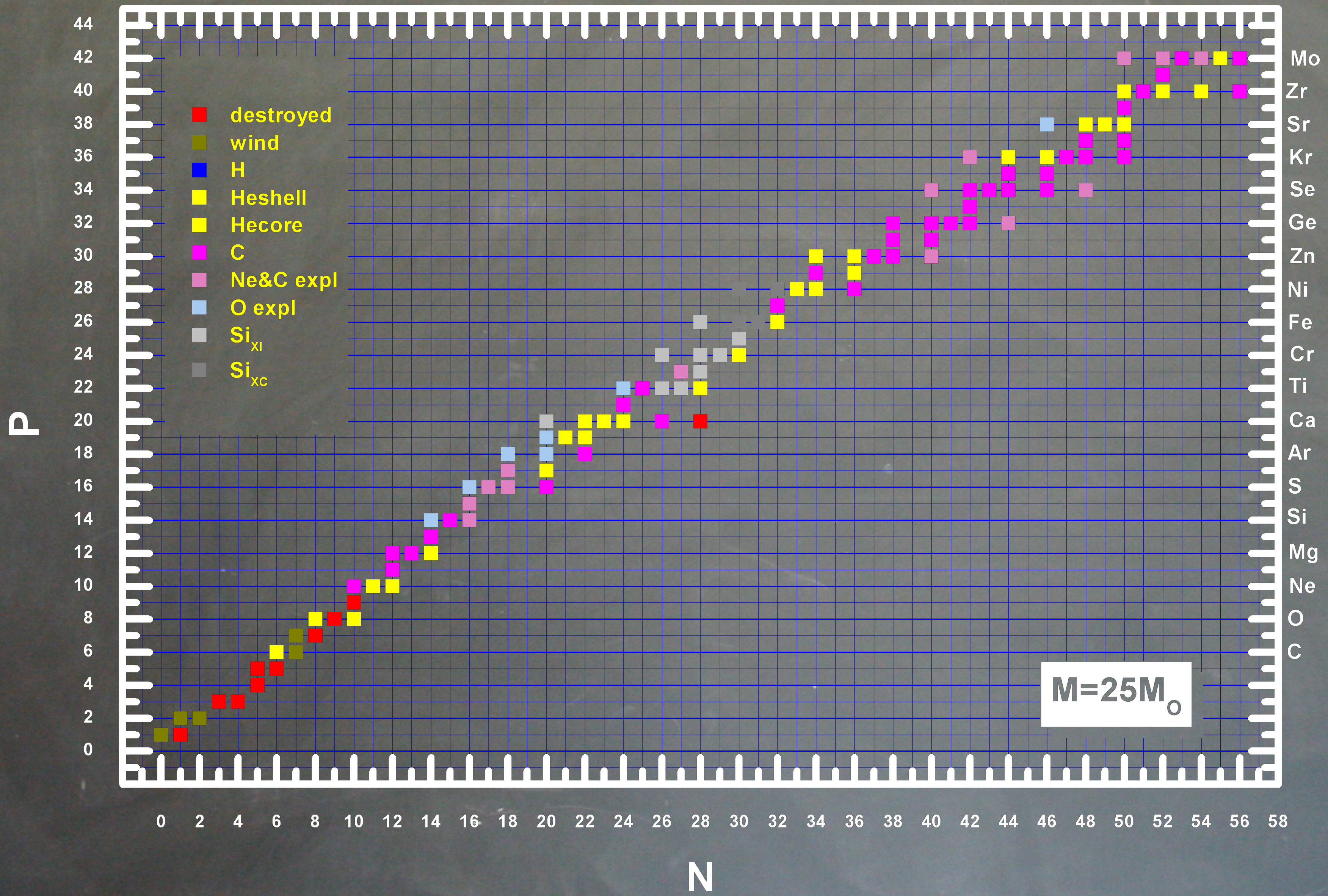
destroyed
wind
H
Heshell
Hecore
C
Ne&C expl
O expl
Si_{XI}
Si_{XC}
$M=25M_O$
P
N
Mo
Zr
Sr
Kr
Se
Ge
Zn
Ni
Fe
Cr
Ti
Ca
Ar
S
Si
Mg
Ne
O
C

Which is the role of the advanced burning phases in the yield production?

shape the final mass – radius relation

influence the explosive yields

model the final Ye profile

Determine the C&Ne abundances in the C convective shell

determine the size of the “Fe” core

Through the extension of the Si convective shell

Determine the final abundances of the nuclei produced by the quiescent C burning: i.e. Ne, Na, Mg, Al + weak S process nucleosynthesis

FRANEC 6.0

Major improvements compared to the release 4.0 (Limongi & Chieffi 2003, Chieffi & Limongi 2004) and 5.0 (Limongi & Chieffi 2006)

- **FULL COUPLING of: Physical Structure - Nuclear Burning -**
  + Chemical Mixing (convection, semiconvection, rotation)

- **INCLUSION OF ROTATION: Transport of Angular Momentum (Advection/Diffusion)**

- **MASS LOSS (Enhanced mass loss for RSG phase, Van Loon 2005)**

- **TWO NUCLEAR NETWORKS:**
  163 isotopes (448 reactions) H/He Burning
  282 isotopes (2928 reactions) Advanced Burning

- **SOLAR COMPOSITION (Asplund et al. 2009)**

FRANEC 6: current release 6.100503

$$\frac{dP}{dM_\Psi} = -\frac{G M_\Psi}{4\pi r_\Psi^4} \cdot f_P \qquad f_P = \frac{4\pi r_\Psi^4}{G M_\Psi S_\Psi < g_{eff}^{-1} >}$$

$$\frac{dM}{dr_\Psi} = 4\pi r_\Psi^2 \rho$$

$$f_T = \frac{16\pi^2 r_\Psi^4}{S_\Psi^2 < g_{eff}^{-1} > < g_{eff} >}$$

$$\frac{d\,lnT_\Psi}{d\,lnP_\Psi} = \frac{3\kappa_\Psi L_\Psi P_\Psi}{16\pi a c G T_\Psi^4 M_\Psi} \cdot \frac{f_T}{f_p}$$

$$dL = \epsilon_\Psi \Delta M$$

$$\rho \frac{d}{dt}(r^2 \omega)_{M_r} = 0$$

$$\frac{d Y_i}{d t} = \left(\frac{\partial Y_i}{\partial t}_{nuc}\right) + \frac{\partial}{\partial m}\left[(4\pi \rho r^2)^2 (D_{semi} + D_{mix} + D_{rot}) \frac{\partial x_i}{\partial m}\right] \qquad i = 1 \ldots N$$

$$1\, system\, of\; M_{meshes} \cdot (N_{isotopes} + 5)\, ODEs$$

$$\rho \frac{d}{dt}(r^2 \omega)_{M_r} = \frac{1}{5}\frac{1}{r^2}\frac{\partial}{\partial r}(\rho r^4 \omega U) + \frac{1}{r^2}\frac{\partial}{\partial r}\left(\rho r^4 D_{shear} \frac{\partial \omega}{\partial r}\right)$$

U(Maeder & Zahn 1998)

← $4\;\;ODEs$

or

$$\rho \frac{d}{dt}(r^2 \omega)_{M_r} = \frac{1}{r^2}\frac{\partial}{\partial r}\left[\rho r^4 \left(D_{shear} + \frac{1}{30} r|U|\right)\frac{\partial \omega}{\partial r}\right]$$

U(Kippenhahn & Weigert 1990)

25 M_{O} - $Z=Z_{O}$

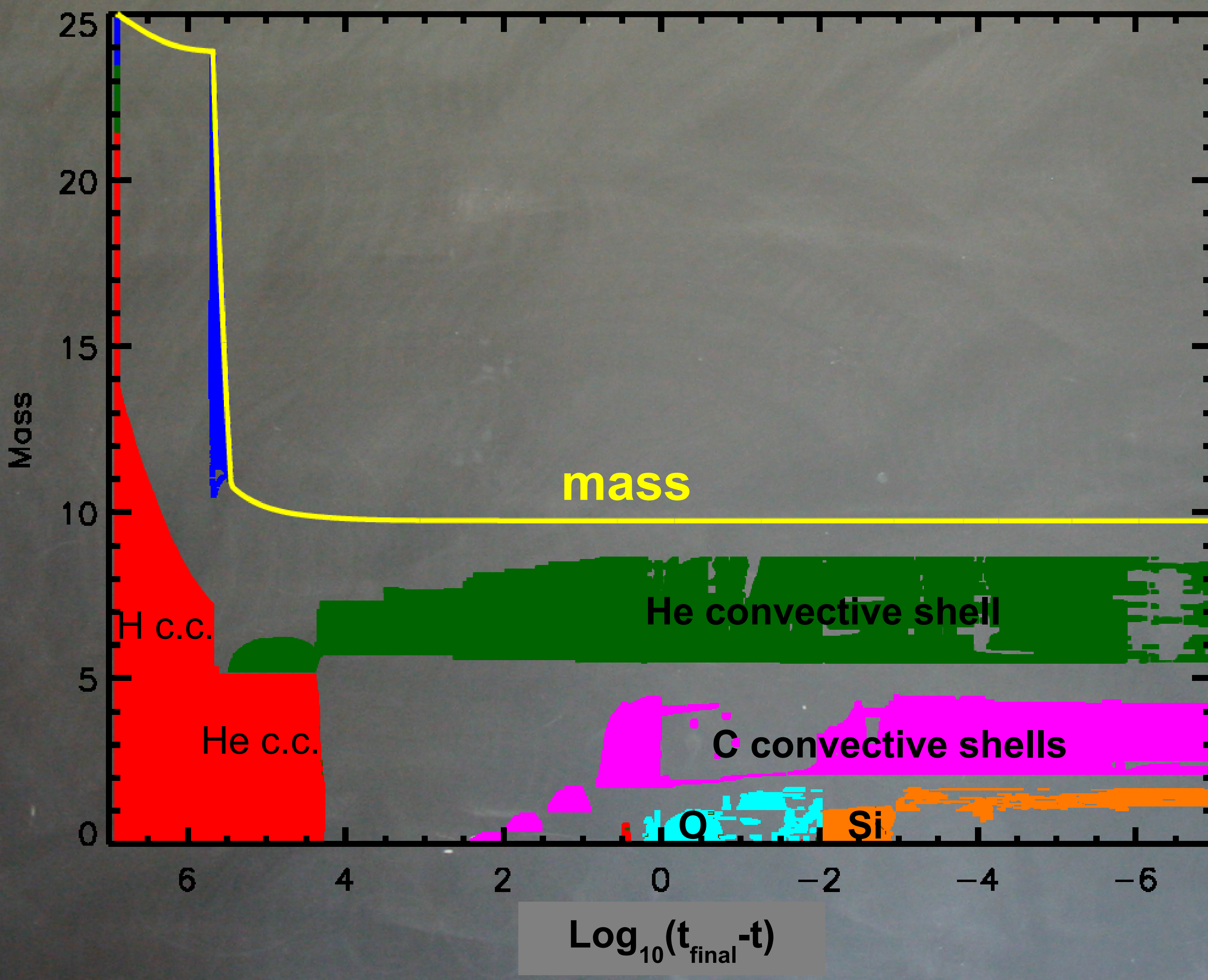

25
20
15
10
5
0
Mass
mass
H c.c.
He c.c.
He convective shell
C convective shells
O
Si
6
4
2
0
−2
−4
−6
Log10(tfinal-t)

Initial equatorial velocity 300 Km/s

25 M_O - $Z=Z_O$

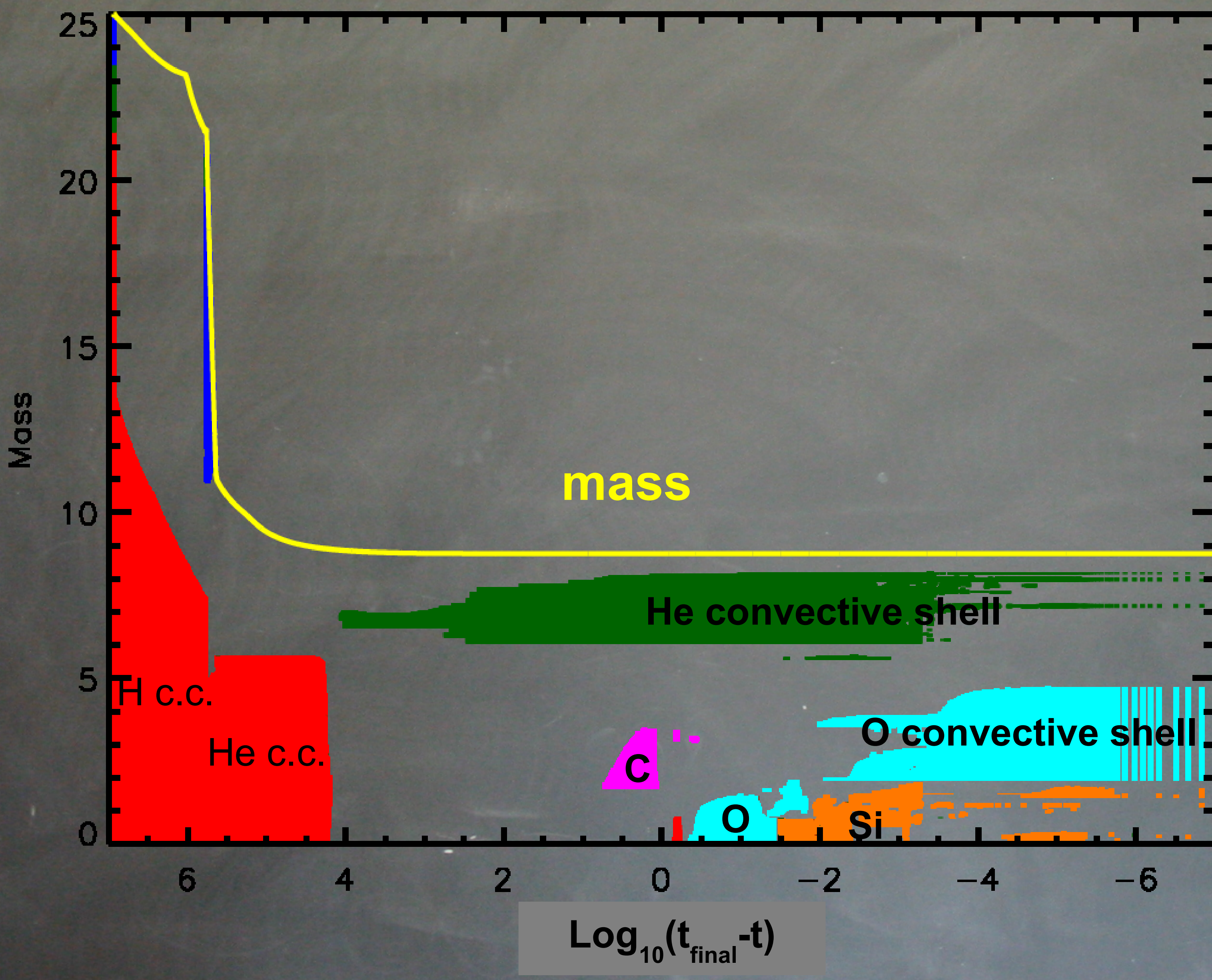

25 $M_{\odot}$ - $Z=Z_{\odot}$

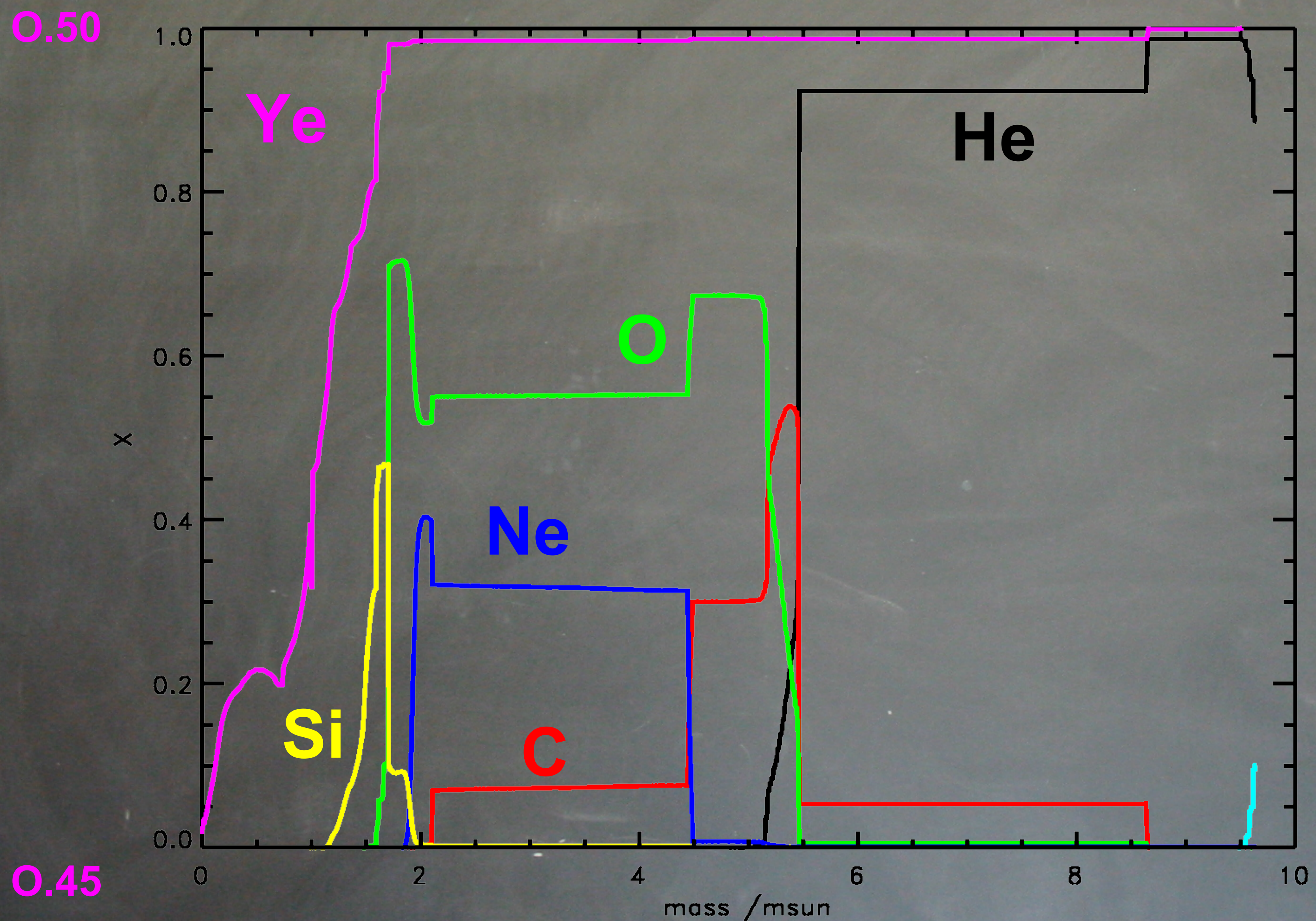

$25\ M_\odot$ - $Z=Z_\odot$

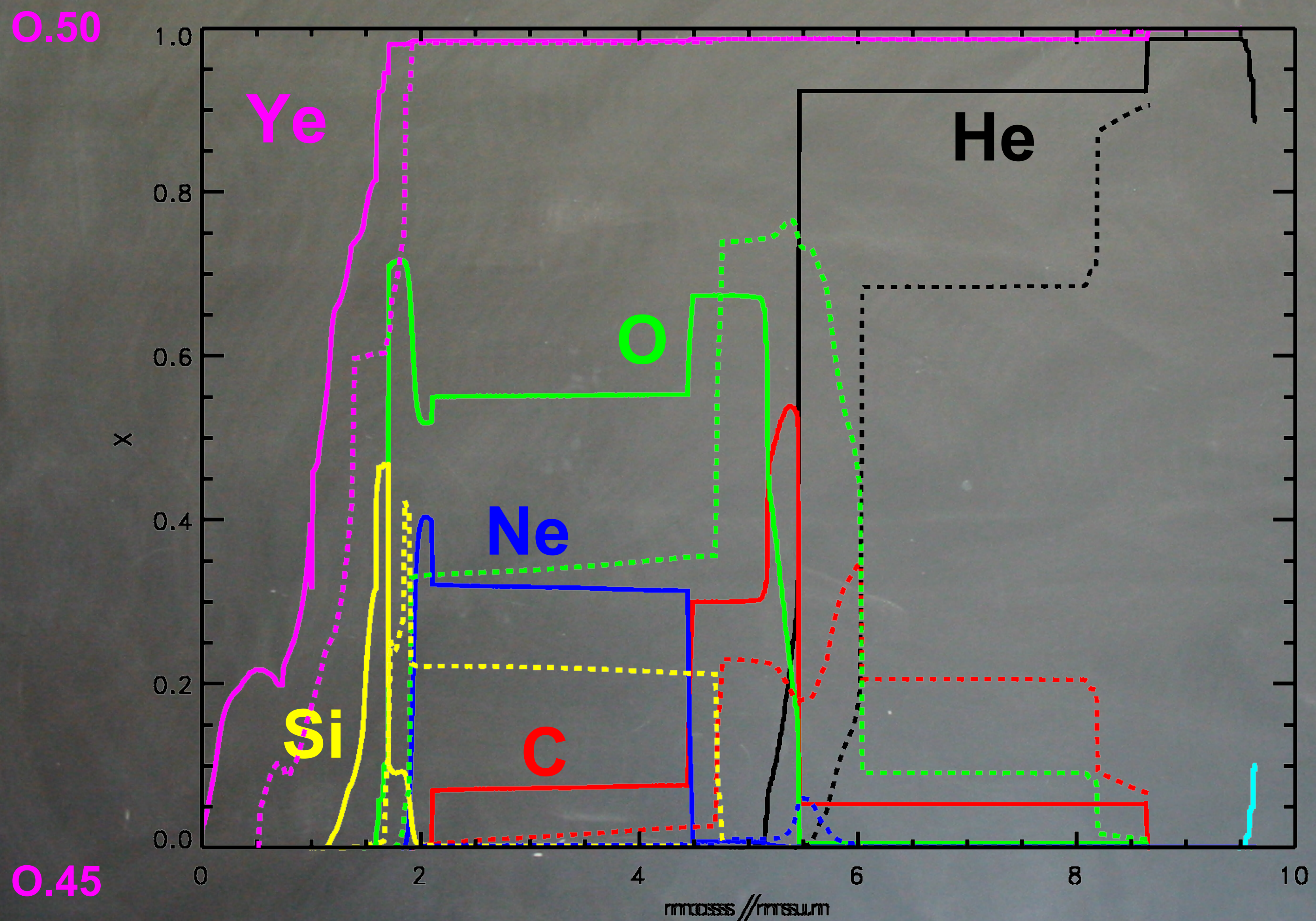

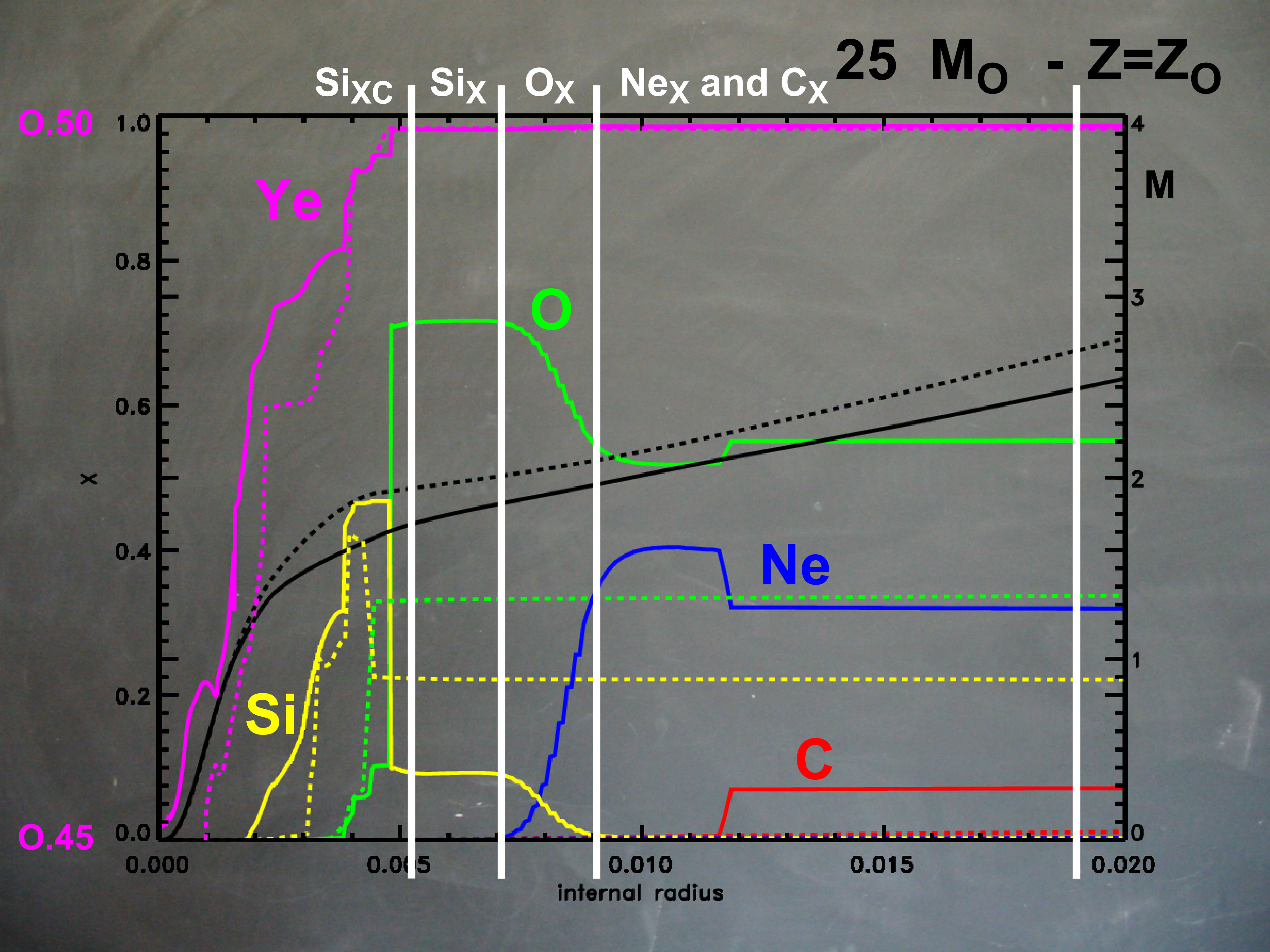
25 MO - Z=ZO
SiXC
SiX
OX
NeX and CX
0.50
0.45
1.0
0.8
0.6
0.4
0.2
0.0
x
Ye
O
Ne
Si
C
M
4
3
2
1
0
0.000
0.005
0.010
0.015
0.020
internal radius